Generalized three-dimensional windowed fourier transform for fringe analysis

Qian, Kemao; Fu, Yu; Liu, Qi; Seah, Hock Soon; Anand, Asundi

2006

Qian, K., Fu, Y., Liu, Q., Seah, H. S., & Asundi, A. (2006). Generalized three-dimensional windowed Fourier transform for fringe analysis. Optics Letters, 31(14), 2121-2123.

https://hdl.handle.net/10356/92141

https://doi.org/10.1364/OL.31.002121

Generalized three-dimensional windowed Fourier transform for fringe analysis

Kemao Qian

School of Computer Engineering, Nanyang Technological University, Singapore, 639798

Yu Fu

Department of Mechanical Engineering, National University of Singapore, 10 Kent Ridge Crescent, Singapore, 119260

Qi Liu and Hock Soon Seah

School of Computer Engineering, Nanyang Technological University, Singapore, 639798

Anand Asundi

School of Mechanical and Aerospace Engineering, Nanyang Technological University, Singapore, 639798

Received February 23, 2006; revised April 17, 2006; accepted April 24, 2006; posted April 26, 2006 (Doc. ID 68342)

A 3D windowed Fourier transform is proposed for fringe sequence analysis, which processes the joint spatial and temporal information of the fringe sequence simultaneously. The 2D windowed Fourier transform in the spatial domain and the 1D windowed Fourier transform in the temporal domain are two special cases of the proposed method. The principles of windowed Fourier filtering and windowed Fourier ridges are developed. Experimental verification shows encouraging results despite a longer processing time. © 2006 Optical Society of America

OCIS codes: 120.2650, 100.2650, 100.5070, 100.7410, 120.3940.

Fringe pattern analysis, or interferogram analysis, is an essential part of optical metrology.[1] Various techniques, such as phase shifting, Fourier transform, regularized phase tracking,[2] and vortex transform,[3,4] have been developed for fringe pattern analysis. Two-dimensional windowed Fourier transform is a novel alternative developed recently.[5–7] To measure a dynamic phenomenon, a fringe sequence is often recorded by using a high-speed camera. Fringe sequences can be processed frame by frame by using existing techniques for fringe pattern analysis, as shown in Fig. 1(a). However, if useful information, such as a temporal carrier is available between consecutive frames, these frames should be processed simultaneously rather than separately.[8] The frames are usually processed pixel by pixel, as shown in Fig. 1(b). As the joint spatial–temporal information could be richer than pure spatial or pure temporal information, a generalized 3D windowed Fourier transform (WFT) is proposed in this Letter. It can be used as a spatial domain method and as a temporal domain method as two special cases. It is interesting to note that the joint information has already been utilized with a Fourier transform.[9] General n-dimensional quadrature transform was also investigated recently, with which a single closed fringe pattern or a temporal set can be successfully demodulated.[10,11] Compared with Fourier transform, vortex transform, and quadrature transform, WFT provides a redundant and localized basis, which is useful for fringe pattern representation and excellent noise reduction.[7]

A 3D fringe sequence can be expressed as

$$f(\vec{r}) = a(\vec{r}) + b(\vec{r})\cos[\varphi(\vec{r})], \tag{1}$$

where $\vec{r}=[x\ y\ t]^T$ is a vector in 3D space with x and y as spatial coordinates and t as the temporal coordinate; T is a transpose operator; $f(\vec{r})$ is the recorded intensity; $a(\vec{r})$ and $b(\vec{r})$ are the background intensity and fringe amplitudes, respectively, which usually vary slowly; and $\varphi(\vec{r})$ is the phase distribution to be determined. In a small volume around a point $\vec{r}_0$, the phase can be approximated as a superplane by Taylor expansion

$$\varphi(\vec{r}) \approx \varphi(\vec{r}_0) + [\nabla\varphi(\vec{r}_0)]^T(\vec{r}-\vec{r}_0), \tag{2}$$

where $\vec{r}$ and $\vec{r}_0$ are two adjacent points with small Euclidean distance and $\nabla\varphi(\vec{r}_0)$ is the gradient of φ at the point $\vec{r}_0$

$$\nabla\varphi(\vec{r}_0) = \left[\left.\frac{\partial\varphi(\vec{r})}{\partial x}\right|_{\vec{r}=\vec{r}_0} \left.\frac{\partial\varphi(\vec{r})}{\partial y}\right|_{\vec{r}=\vec{r}_0} \left.\frac{\partial\varphi(\vec{r})}{\partial t}\right|_{\vec{r}=\vec{r}_0} \right]^T. \tag{3}$$

These are the local angular frequencies or instantaneous angular frequencies at point $\vec{r}_0$. Consequently

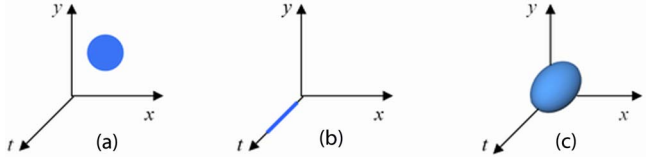

Fig. 1. (Color online) Strategies for fringe analysis. (a) Processing in xy plane (spatial domain), one frame at a time; (b) processing along t axis (temporal domain), one pixel at a time; (c) processing in xyt space (joint spatial-temporal domain).

0146-9592/06/142121-3/$15.00

in the local volume we have

$$\cos[\varphi(\vec{r})] \approx \cos\{\varphi(\vec{r}_0) + [\nabla\varphi(\vec{r}_0)]^T(\vec{r}-\vec{r}_0)\} = \frac{1}{2}\exp\{j\varphi(\vec{r}_0) + j[\nabla\varphi(\vec{r}_0)]^T(\vec{r}-\vec{r}_0)\} + \frac{1}{2}\exp\{-j\varphi(\vec{r}_0) - j[\nabla\varphi(\vec{r}_0)]^T(\vec{r}-\vec{r}_0)\}, \tag{4}$$

where $j=\sqrt{-1}$. Hence in a local volume, $\cos[\varphi(\vec{r})]$ can be effectively represented by harmonics with limited extensions as

$$h(\vec{r};\vec{\xi}) = g(\vec{r})\exp(j\vec{\xi}^T\vec{r}), \tag{5}$$

where $\vec{\xi}=[\xi_x\ \xi_y\ \xi_t]^T$ is a vector of spatial and temporal angular frequency components, $\exp(j\vec{\xi}^T\vec{r})$ is a harmonic with $\vec{\xi}$ as its frequency, and $g(\vec{r})$ is a window that limits the extensions of the harmonic to be in a local volume.

Fortunately all these harmonics with limited extensions construct a basis. To represent a signal by this basis is the essence of the WFT, which has been investigated for the 2D case in our previous work.[5–7] For fringe sequence analysis, the transform is extended to be 3D and is explored in this Letter. This will be shown to be a simple but significant and elegant generalization of the 2D transform.

The window function is chosen as a Gaussian and consequently the kernel of the WFT is

$$h(\vec{r};\vec{\xi}) = \exp\left[-\frac{1}{2}\vec{r}^T K^{-1}\vec{r} + j\vec{\xi}^T\vec{r}\right], \tag{6}$$

where

$$K^{-1} = \begin{bmatrix} 1/\sigma_x^2 & 0 & 0 \\ 0 & 1/\sigma_y^2 & 0 \\ 0 & 0 & 1/\sigma_t^2 \end{bmatrix};$$

σ_x, σ_y, and σ_t are the standard deviation of the Gaussian function and represent the extensions of the harmonics in the x, y, and t axes, respectively. The 3D WFT and inverse transform can be expressed concisely as convolutions

$$f(\vec{r}) = \frac{1}{8\pi^3}\int_{-\infty}^{\infty}\int_{-\infty}^{\infty}\int_{-\infty}^{\infty}\{[f(\vec{r})\otimes h(\vec{r};\vec{\xi})] \otimes h(\vec{r};\vec{\xi})\}\mathrm{d}\xi_x\mathrm{d}\xi_y\mathrm{d}\xi_t, \tag{7}$$

where $f(\vec{r})\otimes h(\vec{r};\vec{\xi})$ is the windowed Fourier spectrum; the symbol $\otimes$ denotes a 3D convolution as

$$a(\vec{r})\otimes b(\vec{r}) = \int_{-\infty}^{\infty}\int_{-\infty}^{\infty}\int_{-\infty}^{\infty} a(u,v,\tau) \times b(x-u,y-v,t-\tau)\mathrm{d}u\mathrm{d}v\mathrm{d}\tau. \tag{8}$$

The above 3D WFT becomes a 2D WFT in the spatial domain when $\sigma_t\to 0$. Similarly it becomes a 1D WFT along the temporal axis when $\sigma_x\to 0$ and $\sigma_y\to 0$.

Based on 3D WFT described above, two algorithms, windowed Fourier filtering (WFF) and windowed Fourier ridges (WFR), are developed. The WFF algorithm is expressed as

$$\bar{f}(\vec{r}) = \frac{1}{8\pi^3}\int_{\xi_{tl}}^{\xi_{th}}\int_{\xi_{yl}}^{\xi_{yh}}\int_{\xi_{xl}}^{\xi_{xh}}\overline{[f(\vec{r})\otimes h(\vec{r};\vec{\xi})]} \otimes h(\vec{r};\vec{\xi})\mathrm{d}\xi_x\mathrm{d}\xi_y\mathrm{d}\xi_t. \tag{9}$$

This equation is very similar to Eq. (7), except for two modifications. First, $\overline{[f(\vec{r})\otimes h(\vec{r};\vec{\xi})]}$ denotes that the original spectrum of $f(\vec{r})\otimes h(\vec{r};\vec{\xi})$ is altered. Usually the spectrum is thresholded such that the spectrum coefficients with small absolute values are set to zero. By this operation, noise can be greatly reduced. Second, the integration is carried out in a selected volume $[\xi_{xl},\xi_{xh}]\times[\xi_{yl},\xi_{yh}]\times[\xi_{tl},\xi_{th}]$ instead of the whole frequency space. This operation selects the desired spectrum sidelobe for signal reconstruction such that an analytic signal is constructed and phase distribution can be extracted. A carrier frequency is desired to avoid the phase ambiguity problem.[12] This operation also reduces computing time.

The WFR algorithm is expressed as

$$\nabla\varphi(\vec{r}) = \arg\max_{\vec{\xi}}|f(\vec{r})\otimes h(\vec{r};\vec{\xi})|, \tag{10}$$

which means that $\nabla\varphi(\vec{r})$ takes the value of $\vec{\xi}$ when this $\vec{\xi}$ maximizes the amplitude spectrum $|f(\vec{r})\otimes h(\vec{r};\vec{\xi})|$. In this algorithm, $h(\vec{r};\vec{\xi})$ with different $\vec{\xi}$ are generated and compared with the signal in a local volume around a point $\vec{r}_0$. The highest similarity (best match) is found and named as a ridge. The value of $\vec{\xi}$ for the best match is selected to represent the gradient of the phase at the point $\vec{r}_0$.The gradient of the phase at any other points $\vec{r}$ can be determined by the same matching process. The phase can be obtained by integrating $\nabla\varphi(\vec{r})$, or can be determined as

$$\varphi(\vec{r}) = \mathrm{angle}\{f(\vec{r})\otimes h[r;\nabla\varphi(\vec{r})]\}. \tag{11}$$

To verify the proposed concept, an electronic speckle pattern interferometry fringe sequence on a continuously deforming plate with an artificial defect (a circular blind hole) is recorded and processed. The plate is loaded by compressed air and deformed in one direction by increments of pressure. A temporal carrier is provided by the deformation itself. The sequence contains 150 frames with a frame size of 220 pixels $\times$220 pixels. The gray level is from 0 to 255. Four frames (frames 31, 61, 91, and 121) from the sequence are shown in the first row of Fig. 2. The second row of Fig. 2 shows the wrapped phase maps obtained by using the WFF algorithm shown in Eq. (9), where $\sigma_x=10$ pixels, $\sigma_y=10$ pixels, and $\sigma_t=5$ frames. The spectrum sidelobe is $[\xi_{xl},\xi_{xh}]\times[\xi_{yl},\xi_{yh}]\times[\xi_{tl},\xi_{th}] = [-0.8,0.8]\times[-0.8,0.8]\times[0.2,0.7]$. Their units are radian/pixel, radian/pixel, and radian/frame, respec-

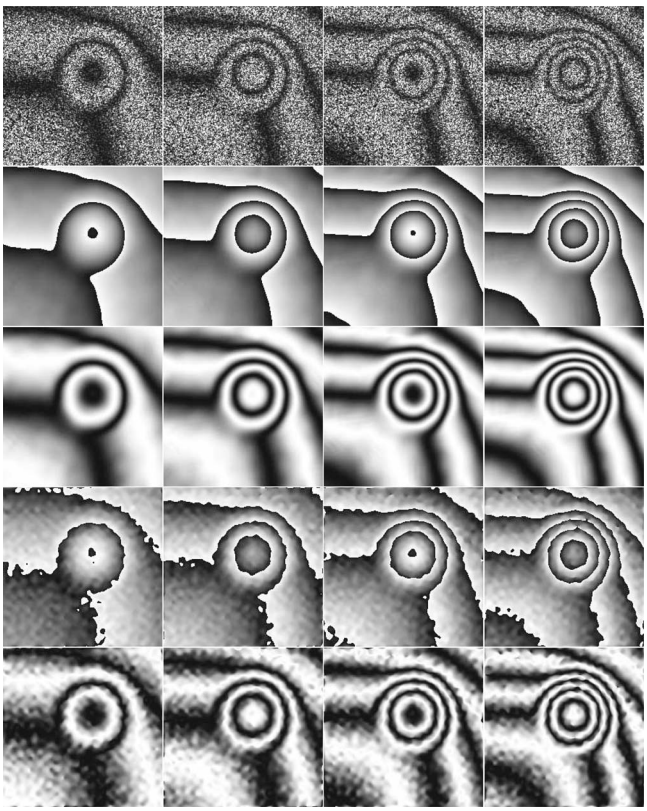

Fig. 2. Fringe sequence analysis by WFT and Fourier transform (FT). First row, four frames from a fringe sequence; second row, extracted phase using WFT; third row, cosine value of the extracted phase in the second row; fourth row, extracted phase using FT; last row, cosine value of the extracted phase in the fourth row.

tively. The sampling rates are $\Delta\xi_x = 0.05$ rad/pixel, $\Delta\xi_y = 0.05$ rad/pixel, and $\Delta\xi_t = 0.1$ rad/frame, respectively. The threshold is empirically set to be 600. The phase can be easily unwrapped. For ease of comparison, the obtained phase data $\varphi(\vec{r})$ is converted to cosine fringes, as shown in the third row of Fig. 2. It can be seen that the result is satisfactory. It is worth noting that no preprocessing and postprocessing are needed. For comparison, the fourth row shows the best estimation we could obtain by using a 3D Fourier transform. Similarly, the corresponding cosine fringes are shown in the last row. The improvement of WFT over the Fourier technique is obvious.

Though the 3D WFT results in 6D spectrum coefficients, it is not necessary to store all these coefficients. Take the WFF in Eq. (9) as an example: for a specific frequency $\vec{\xi}$, its spectrum coefficient can be computed as $f(\vec{r}) \otimes h(\vec{r}; \vec{\xi})$, which is thresholded and used for reconstructing the signal $\bar{f}(\vec{r})$. This spectrum coefficient can then be discarded. Another frequency is selected for the same processing until all the sampled frequencies are computed. For the above example, approximately 150 Mbytes of memory are needed to store the original sequence, the temporary spectrum, and the reconstructed sequence with single precision. Hence the requirement for memory is not very high. However, the 3D transform does need a long computing time. For the above example, 7 h are consumed to obtain the phase information by using the C language on a Pentium IV 3.2 GHz processor with hyperthreading. As a reference, the time for the 3D Fourier transform is less than 1 s. This is because two 3D convolutions, one for analysis and the other for synthesis, are needed for each sampled frequency in WFF, as shown in Eq. (9). However, this heavy burden can be reduced by the rapid development of computing technology, such as parallel computing techniques.[13]

The authors thank the reviewers for their insightful and helpful comments. K. Qian's e-mail address is mkmqian@ntu.edu.sg.

References

1. D. W. Robinson and G. T. Reid, eds., *Interferogram Analysis: Digital Fringe Pattern Measurement Techniques* (Institute of Physics, 1993).
2. M. Servin and M. Kujawinska, in *Handbook of Optical Engineering*, D. Malacara and B. J. Thompson, eds. (Marcel Dekker, 2001).
3. K. G. Larkin, D. J. Bone, and M. A. Oldfield, J. Opt. Soc. Am. A **18**, 1862 (2001).
4. K. G. Larkin, J. Opt. Soc. Am. A **18**, 1871 (2001).
5. K. Qian, Appl. Opt. **43**, 2695 (2004).
6. K. Qian, Appl. Opt. **43**, 3472 (2004).
7. K. Qian, Opt. Lasers Eng. (to be published).
8. Y. Fu, C. J. Tay, C. Quan, and H. Miao, Appl. Opt. **44**, 959 (2005).
9. M. Takeda and M. Kitoh, J. Opt. Soc. Am. A **9**, 1607 (1992).
10. M. Servin, J. A. Quiroga, and J. L. Marroquin, J. Opt. Soc. Am. A **20**, 925 (2003).
11. J. A. Quiroga, M. Servin, J. L. Marroquin, and D. Crespo, J. Opt. Soc. Am. A **22**, 439 (2005).
12. M. Takeda, H. Ina, and S. Kobayashi, J. Opt. Soc. Am. **72**, 156 (1982).
13. T. W. Ng, K. T. Ang, and G. Argentini, Appl. Opt. **44**, 7125 (2005).